Peeling bifurcations of toroidal chaotic attractors

Christophe Letellier,[1] Robert Gilmore,[1,2] and Timothy Jones[2]
[1]*CORIA UMR 6614—Université de Rouen, Av. de l'Université, Boîte Postale 12, F-76801 Saint-Etienne du Rouvray cedex, France*
[2]*Physics Department, Drexel University, Philadelphia, Pennsylvania 19104, USA*
(Received 12 July 2007; published 11 December 2007)

Chaotic attractors with toroidal topology (van der Pol attractor) have counterparts with symmetry that exhibit unfamiliar phenomena. We investigate double covers of toroidal attractors, discuss changes in their morphology under correlated peeling bifurcations, describe their topological structures and the changes undergone as a symmetry axis crosses the original attractor, and indicate how the symbol name of a trajectory in the original lifts to one in the cover. Covering orbits are described using a powerful synthesis of kneading theory with refinements of the circle map. These methods are applied to a simple version of the van der Pol oscillator.

DOI: 10.1103/PhysRevE.76.066204 PACS number(s): 05.45.−a

I. INTRODUCTION

It has been known for some time that discrete symmetry groups can be used to relate chaotic attractors with different global topological structures [1–4]. By different (or distinct) topological structures we mean there is no smooth deformation of the phase space that can be used to transform one attractor into the other in a smooth way. If a chaotic attractor has a discrete symmetry, points in the attractor that are mapped into each other under the discrete symmetry can be identified with a single point in an "image" attractor. The identifications are through local diffeomorphisms. The original symmetric attractor and its image are not globally topologically equivalent. This process can be run in reverse. A chaotic attractor without symmetry can be "lifted" to a covering attractor with a discrete symmetry following algorithmic procedures [1–5].

A simple example illustrates these ideas. The Lorenz attractor [6] obtained with standard control parameter values exhibits a twofold symmetry. The symmetry is generated by rotations about the Z axis through π radians: $R_Z(\pi)$. We mod out this twofold symmetry by identifying pairs of points (X,Y,Z) and $(-X,-Y,Z)$ in the symmetric attractor with a single point $(u,v,w)=(X^2-Y^2,2XY,Z)$ in the image attractor. This results in a chaotic attractor that is not topologically equivalent to the original attractor. Rather, it is topologically equivalent (not diffeomorphic [1,2,4]) with the Rössler attractor [7]. Similarly, the Rössler attractor can be lifted to a twofold covering attractor that is topologically equivalent to the Lorenz attractor. The lift is carried out by inverting the $2\rightarrow 1$ local diffeomorphism used to generate the image: $(u,v,w)\rightarrow\left[X=\pm\sqrt{\frac{1}{2}(r+u)},Y=\pm\sqrt{\frac{1}{2}(r-u)},Z=w\right]$, where $r=\sqrt{u^2+v^2}=X^2+Y^2$. This modding out process is illustrated in Fig. 1.

A single image attractor can have many topologically inequivalent covers, all with the same symmetry group. These covers are differentiated by an index [3–5]. The index has interpretations at the topological, algebraic, and group theoretical levels. Briefly, the index describes how the singular set of the local diffeomorphism relating cover and image attractors is situated with respect to the image attractor. Different lifts of the Rössler attractor, all with $R_Z(\pi)$ symmetry but with different indices, are obtained if the twofold rotation axis passes through the hole in the middle of the Rössler attractor, passes through the attractor itself, or passes outside both the attractor and the hole in the middle (cf. Fig. 2). The transition of the symmetry axis through the attractor is responsible for peeling bifurcations [2].

Rössler-type attractors have been lifted to covers with many symmetry groups [5]. Whenever the singular set of the symmetry group involves a rotation axis, this axis has passed through the attractor at most once in all previous studies.

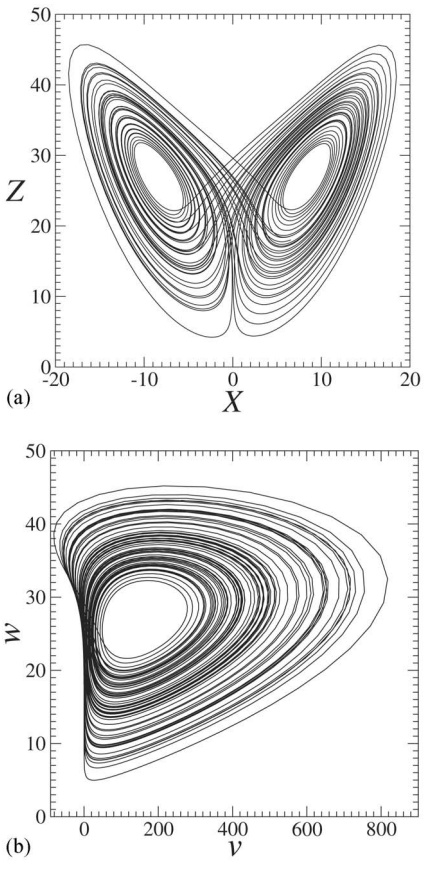

FIG. 1. The Lorenz attractor (a) can be mapped to a Rössler-type attractor (b) by identifying points related by rotation symmetry about the Z axis. This process is reversible: Rössler-type attractors can be "lifted" to Lorenz-type attractors.

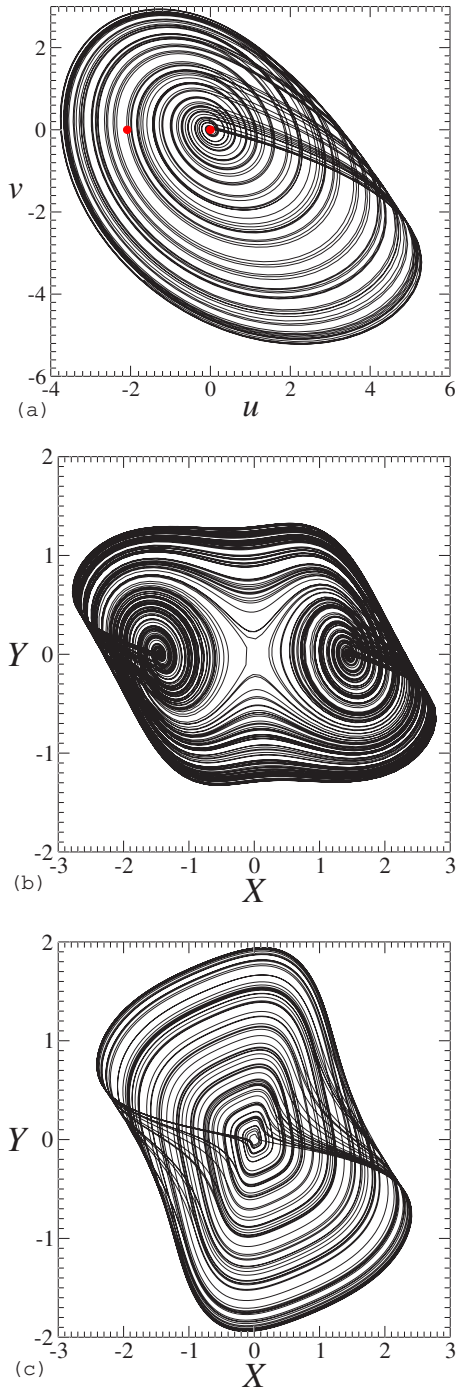

FIG. 2. (Color online) The Rössler attractor (a) can be lifted to topologically distinct double covers with rotation symmetry by placing the rotation axis in different positions: (b) in the attractor; (c) in the hole in the middle of the attractor.

More precisely, it has passed through the branched manifold [8–11] describing the attractor at a single point.

There have been no studies of covering attractors that are obtained when the rotation axis intersects the image attractor in more than one spot. Generically, a rotation axis must intersect a toroidal attractor an even number of times. In the present work we look at twofold covers of toroidal attractors with rotation symmetry. We use methods similar to those used in [1–5]. Many of our results depend on a powerful synthesis of kneading theory with refinements of the circle map.

In Sec. VI below we study peeling bifurcations for rotation-symmetric lifts of a chaotic attractor generated by the van der Pol equations subject to a periodic drive. The phase space of this attractor is a "hollow donut" or "fat tire," that is, the direct product of an annulus with a circle: $A^2 \times S^1$. An annulus itself is a circle with a thick circumference: $A^2 = S^1 \times I$, where I is an interval, or short segment of the real line. The branched manifold that describes this attractor is essentially a torus (thin tire). A rotation axis used to construct symmetric lifts must intersect the torus an even number of times. Lifts of laminar and chaotic flows on a torus are discussed in Secs. IV and V, respectively. The first of these sections describes how the symbolic dynamics of image trajectories lift to symbolic dynamics in covering trajectories. The second describes how the branched manifold describing the image attractor lifts to the branched manifold describing the covering attractor. We prepare for these discussions by introducing toroidal coordinates and describing flows on a torus in Sec. III. We begin this entire odyssey in Sec. II with a review of peeling bifurcations and their properties. Our results are summarized in Sec. VII.

II. REVIEW OF PEELING BIFURCATIONS

Peeling bifurcations arise naturally when considering covers of chaotic attractors. They describe the bifurcations these covers can undergo as the relative position of the image attractor and the symmetry axis changes. Peeling bifurcations have been described in some detail for covers of the Rössler dynamical system in [2,4].

We briefly describe the basic idea for double covers with $R_Z(\pi)$ symmetry about a rotation axis $\mathcal{R}$ with the usual saddle-type symmetry. Lift an image attractor [Fig. 2(a)] to a double cover with $\mathcal{R}$ far away from the original image attractor. The double cover consists of two identical copies of the original image attractor. They are disconnected. An initial condition in one will evolve on that attractor for all future times in the absence of noise. As the rotation axis $\mathcal{R}$ approaches the image the two disjoint components of the double cover approach each other, keeping $\mathcal{R}$ between them. At some point $\mathcal{R}$ will intersect the attractor. When this occurs the rotation axis will split the outer edge of the flow from one of the two components of the cover and send it to the other component, and vice versa. The two attractors in the cover are no longer disconnected [Fig. 2(b)]. As the rotation axis $\mathcal{R}$ moves deeper to the center of the image attractor (towards the center of rotation of the Rössler attractor, for example), the double cover becomes smaller in spatial extent. Finally, the rotation axis $\mathcal{R}$ may stop intersecting the image by passing into the hole in the middle [Fig. 2(c)].

The peeling bifurcation takes place as the rotation axis moves from the outside to the inside of the image attractor. The image attractor itself is not affected. All bifurcations take place in the cover. Before intersections begin and after they end the double covers are structurally stable and topologically inequivalent. During the intersection phase the cover is structurally unstable because slight changes in the

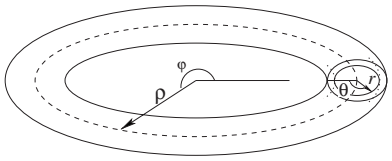

FIG. 3. Coordinates adapted to an annular torus.

position of the rotation axis produce profound changes in lifts of trajectories from the image. That is, a trajectory remains unchanged in the image while its lift(s) into the cover change dramatically as the rotation axis $\mathcal{R}$ moves. Changes in the shape, structure, and period of lifts of unstable periodic orbits from the image into the cover are predictable. These changes are summarized for covers of Rössler-type attractors in Figs. 7–12 of Ref. [2].

It may be useful to regard peeling bifurcations in terms of how two trajectories in the cover that result from the lift of a single trajectory in the image connect or reconnect as the position of the symmetry axis changes. Roughly but accurately, they can "turn back" into the subset of the attractor from which they originated when the axis is outside the trajectory, or else "cross over" into the complement of that subset when the axis is inside the trajectory. This behavior is reminiscent of what happens during the transition of a plane through a saddle point on a surface, with the added feature of "direction." Since orbits are dense in a strange attractor, the lifted system cannot be structurally stable during a peeling bifurcation.

III. FLOWS ON A TORUS

It is useful to describe flows on a torus in terms of a system of coordinates adapted to the torus: (ϕ,θ,r). In such a coordinate system ϕ is the longitude; it increases with time: $d\phi/dt>0$. The angle θ is the meridional angle, measured from "the inside of the torus" (see Fig. 3), and r measures the distance of a point in the annulus $0<r_1\leq r\leq r_2$ at constant angle ϕ from the center line of the torus, a circle of radius ρ in the x-y plane. The circle radius ρ must be sufficiently large so that $\rho-r>0$ for all points in the attractor. Standard Cartesian coordinates are represented in terms of these toroidal coordinates by

$$x=(\rho-r\cos\theta)\cos\phi,$$

$$y=(\rho-r\cos\theta)\sin\phi,$$

$$z=-r\sin\theta. \tag{1}$$

The Birman-Williams theorem [8–11] can be applied to dissipative toroidal flows in $\mathbb{R}^3$ that generate strange attractors. The result is that the topology of the flow is described by a branched manifold. The mechanism generating chaotic behavior involves an even number of folds. The branch "lines" are now circles. Since the flow occurs in a bounding torus [12,13] of genus one, the Poincaré surface of section consists of a single disk. The intersection of the branched manifold with the disk ("branch line") is topologically a circle, S^1. As a result, the flow can be investigated by studying maps of the circle to itself [14].

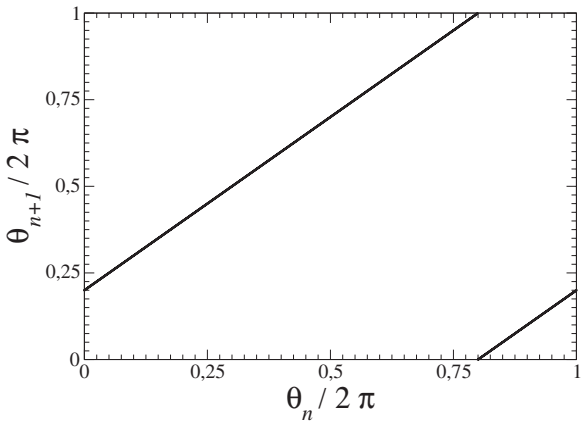

FIG. 4. The return map for a rigid rotation is a straight line mod 2π. $\Omega/2\pi=0.20$.

IV. LIFTS OF RIGID ROTATIONS

In order to determine the topological structure of a strange attractor in $\mathbb{R}^3$ it is sufficient to determine the topological structure of the branched manifold that describes it. This remains true for covers of strange attractors with arbitrary symmetry [4,5,8]. We do this in the following section.

In this section we prepare the groundwork by investigating how a rigid rotational (quasiperiodic) flow on a torus is lifted to a double cover of the torus. This is easily done by setting $\rho=2, r=1, \theta=\alpha\phi$ in the toroidal coordinates. This curve closes or does not close depending on whether α is rational or irrational. The return map on a plane $\phi=$const is shown in Fig. 4. It is $\theta_{n+1}=\theta_n+\Omega \bmod 2\pi$.

Now pass a rotation axis through the torus as shown in Fig. 5. The order-two rotation axis intersects the torus in an interval I. If the rotation axis is parallel to the Z axis, the end points of this interval are at $\theta=2\pi(\frac{1}{2}\pm\sigma)$. The rotation symmetry lifts the torus into a structure inside a genus-three bounding torus that is shown in Fig. 6. The location of the rotation axis is indicated by ×.

Since the flow exists in a bounding torus of genus three the global Poincaré surface of section has two components [12,13]. In such cases the first return map consists of a 2 × 2 array of maps [4,15]. For the Lorenz attractor such maps indicate flows from branch line to branch line. In the present case the return map indicates flows from the branch circles on the left and right of Fig. 7. The return map for the cover of the rigid rotational flow, in the case that the Z axis inter-

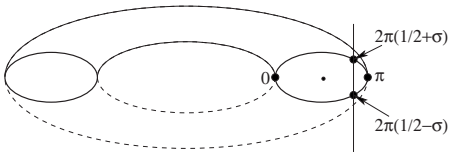

FIG. 5. The order-two rotation axis intersects the torus at $2\pi(\frac{1}{2}\pm\sigma)$.

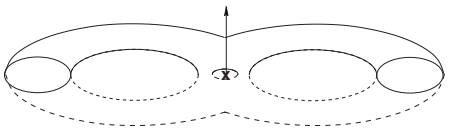

FIG. 6. When the order-two rotation axis intersects the torus at $2\pi\left(\frac{1}{2}\pm\sigma\right)$, the double cover consists of a structure with the topology shown. This geometric structure exists inside a bounding torus of genus three.

sects the image torus at $\theta=\pi\pm 2\pi\sigma$, is presented in Fig. 8. The angles parametrizing the branch circles on the left and right run from zero to 2π. This figure shows that an initial condition within $2\pi\sigma$ of $\theta=\pi$ on the left-hand-branch circle maps to the right-hand-branch circle [see Fig. 8(a)], and vice versa.

A symbol name for any trajectory on the covering flow is easily constructed. Assume the return map in the image is $\theta_{n+1}=\theta_n+\Omega \bmod 2\pi$. Then $\theta_n=\theta_0+n\Omega \bmod 2\pi$. Write out this string of real numbers and replace each value θ_n by 1 if $\theta_n \in I$, zero otherwise. This results in a string of symbols, for example, 00000 11111 00000… for initial condition L. Choose an initial condition L or R, for one side of the cover or the other. Then repeat this letter following symbol 0, conjugate this letter ($L\rightarrow R$, $R\rightarrow L$) following symbol 1. This algorithm leads to 000001111100000… $\rightarrow LLLLLRLRLRRRRRR\ldots$. A rotation-symmetric trajectory has a conjugate sequence.

Depending on parameter values (e.g., $\alpha \ll \sigma < \frac{1}{4}$) the symbol sequence can consist of long strings of Ls, long strings of Rs, and long strings of LRs, giving the appearance of prolonged rotation about three centers: one being the left-hand torus in the lift, another being the right-hand torus in the lift, and the third alternation about both in sequence when θ_n falls in the interval I over a large range of successive interations.

As the rotation axis sweeps from the outside to the inside of the torus, the value of σ increases. The circular intervals for which transition from one side to the other takes place increases, with the return map becoming more and more off-diagonal. As the Z axis approaches the inner part of the image torus, the measure of θ values that map to the same branch circle decreases, and becomes zero when tangency occurs ($\sigma=\pi$). At this point the return map is completely off-diagonal. This is an indication that the global Poincaré surface of section is no longer the union of two disjoint disks. A single disk suffices. This signals that the flow returns to a flow of genus-one type, and the return map on the single disk is $\theta_{n+1}=\theta_n+2\Omega \bmod 2\pi$ (notice the factor of 2).

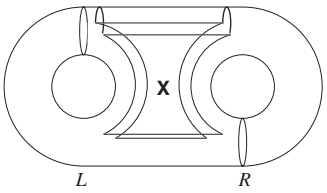

FIG. 7. The laminar flow on a torus lifts to a flow on a manifold with the complicated form shown. The rotation axis is indicated by cross.

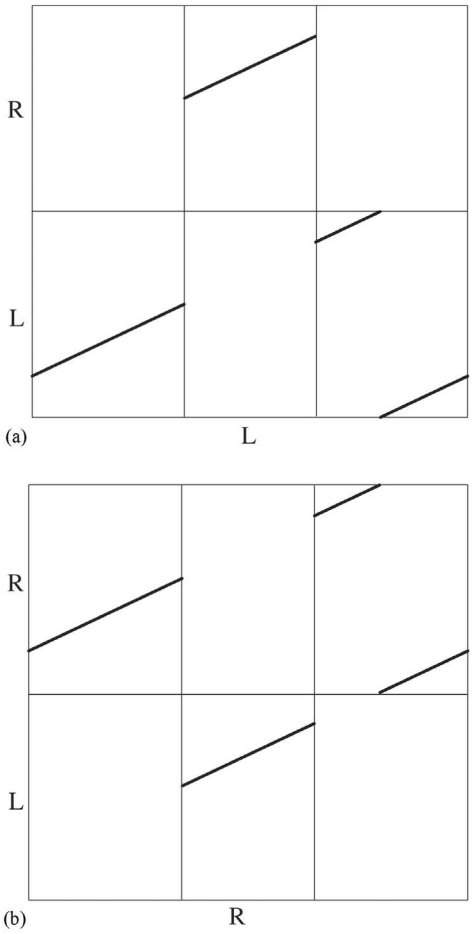

FIG. 8. Return map for a rigid flow contained within a genus-three torus consists of mappings from two branch circles to themselves.

In the limit when the rotation axis is outside the torus ("$\sigma<0$") the double cover consists of two disconnected tori. An initial condition in one torus remains forever in that torus. In the limit when the rotation axis is in the hole in the middle of the torus ("$\sigma>\frac{1}{2}$") the double cover consists of a single torus. When the rotation axis goes through the origin of Cartesian coordinates, the longitudinal angle ϕ in the image increases twice as fast as the longitudinal angle Φ in the cover. Simulations of peeling bifurcations for double and triple covers of laminar flows on a torus can be found in [16].

V. LIFTS OF CHAOTIC ATTRACTORS

There is a class of strange attractors, such as the van der Pol attractor that we discuss in the following section, whose phase space is a hollow donut, topologically $A^2\times S^1$, where S^1 describes the longitudinal (flow) direction. The intersection of the attractor with a constant phase plane ϕ=const occurs in an annulus $A^2=S^1\times I$, where this S^1 describes the meridional direction and I is a small interval. Under the Birman-Williams projection [10,11] the intersection of the projected attractor with the plane ϕ=const is topologically a circle S^1. The forward time map $\phi\rightarrow\phi+2\pi$ is therefore a

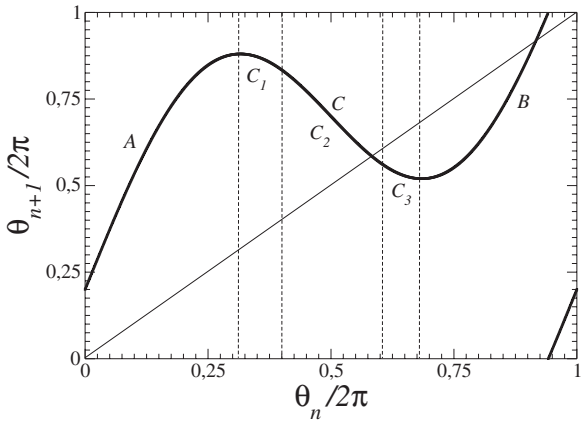

FIG. 9. Circle map Eq. (2) for $K=2.5$, $\Omega/2\pi=0.2$. The three branches are conveniently labeled A, C, B.

mapping of the circle to itself. As a result, many of the properties of this class of attractors are determined by the properties of the circle map. For example, the number and labeling of the branches of the attractor's branched manifold are determined by the appropriate circle map.

For simplicity we assume that three branches A, C, B suffice to describe the branched manifold, and that the return map on the singularity at which these branches are joined (the branch circle) is a circle map [14] as follows:

$$\theta_{n+1} = \theta_n + \Omega + K \sin \theta_n \bmod 2\pi, \tag{2}$$

with $K>1$. This map is shown in Fig. 9. Branch C is orientation reversing. Its forward image extends over a range less than 2π and its extent is delineated by the two critical points. Branches A and B are orientation preserving and their forward image extends over a range greater than 2π. They are delineated by the critical points that bound C and the inflection point between them.

The return map for the double cover is obtained as in the previous section. We begin by looking at intersections of the rotation axis near the outside of the torus, at values $\theta=\pi\pm2\pi\sigma$, with σ small. The return map on the two branch circles is as shown in Fig. 10 for $\sigma=0.15$.

The return map for the double cover is obtained from the return map for the image as follows. The vertical lines through the maximum and the minimum and the vertical axis at $\theta/2\pi=0,1$ in Fig. 9 separate the return map into three branches A, B, C.

The two additional vertical lines separate branch C into three branches: C_2 which is the interval I: $\pi-2\pi\sigma<\theta<\pi+2\pi\sigma$, and C_1 and C_3, which map $L\to L$ and $R\to R$. Generally there are no degeneracies, so these five vertical lines divide the circle into five angular intervals. In the present case both endpoints of the interval I occur inside the orientation-reversing branch C, so this branch is divided into three parts: C_1, C_2, C_3, as shown in Fig. 9. As a result, initial conditions on branches A and B, and the adjacent parts of branch C, namely, C_1 and C_3 of the circle on the left, map back to that circle while initial conditions in the angular interval C_2 on the left circle map to the right-hand circle. The

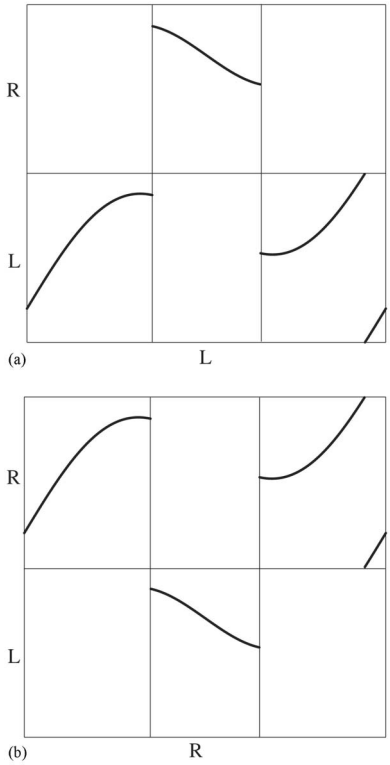

FIG. 10. Return map for the double cover of the chaotic flow whose return map is shown in Fig. 9. Parameter value: $\sigma=0.15$.

branched manifold describing the covering flow has ten branches with transitions summarized as follows:

$L\to L$	$R\to R$	$L\to R$	$R\to L$
A	A		
C_1	C_1		
		C_2	C_2
C_3	C_3		
B	B		

In the event that one (both) of the endpoints of the interval I coincide with one (two) of the three points separating A, C, B there are eight (six) branches.

Before the peeling bifurcation begins, when the two identical covers are well separated, each is characterized by a branched manifold with three branches. At the end of the peeling bifurcation, when the rotation axis $\mathcal{R}$ is inside the image torus, there are $9=3^2$ branches that can be labeled $(A,C,B)\otimes(A,C,B)=[AA,BA,CA,AB,BB,CB,CA,CB,CC]$ [2,3]. Branches labeled by an even number of letters C are orientation preserving.

A periodic orbit in the image can be lifted to one or two covering orbits. The symbol name of the covering orbit is obtained from the symbol name of the image orbit and information about the interval I. The name of the orbit in the image is written out (e.g., $ABBCBBAC$) and refined according to the location of the interval I (e.g., $ABBC_2BBAC_3$). An initial condition on the left or right (L or R) is given and this is changed whenever a trajectory passes through

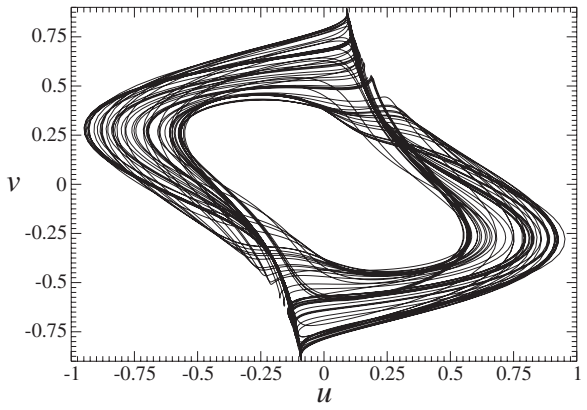

FIG. 11. Projections of the van der Pol attractor on the plane u-v. Parameter values: $(a,b,c,d,\omega)=(0.25,0.7,1.0,10.0,\pi/2)$.

one of the branches defined by I. For example, under this algorithm $ABBCBBAC \rightarrow A_L B_L B_L C_{2L} B_L B_L A_L C_{3L} A_R B_R B_R C_{2R} B_R B_R A_R C_{3R}$. A period-$p$ orbit lifts to two period-p orbits or one symmetric orbit of period $2p$ depending on whether the image orbit maps through the interval I an even or odd number of times. The algorithm for lifting orbits from a toroidal flow to a double cover involves a synthesis of kneading theory with refinement of the circle map due to the intersection of the rotation axis with the image toroidal flow.

VI. APPLICATION TO THE VAN DER POL ATTRACTOR

The Shaw version [17] of the periodically driven van der Pol equations

$$\dot{u} = bv + (c - dv^2)u,$$

$$\dot{v} = -u + a\sin(\omega t), \tag{3}$$

produce a toroidal attractor for control parameter values $(a,b,c,d,\omega)=(0.25,0.7,1.0,10.0,\pi/2)$ [4,9]. The phase space for this attractor is the direct product of an annular disk with a circle. One projection of this attractor is shown in Fig. 11.

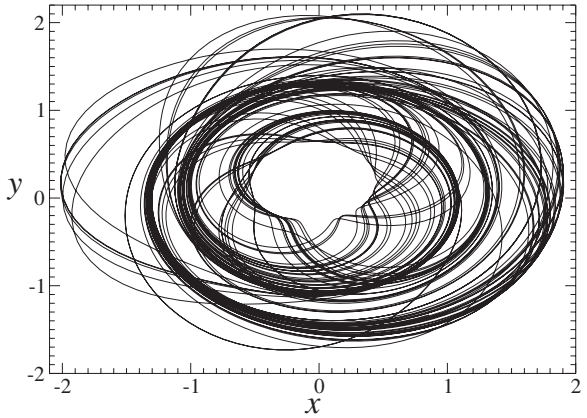

FIG. 12. Mapping of the van der Pol attractor into R^3 using Eq. (1) with $\rho=1.2$.

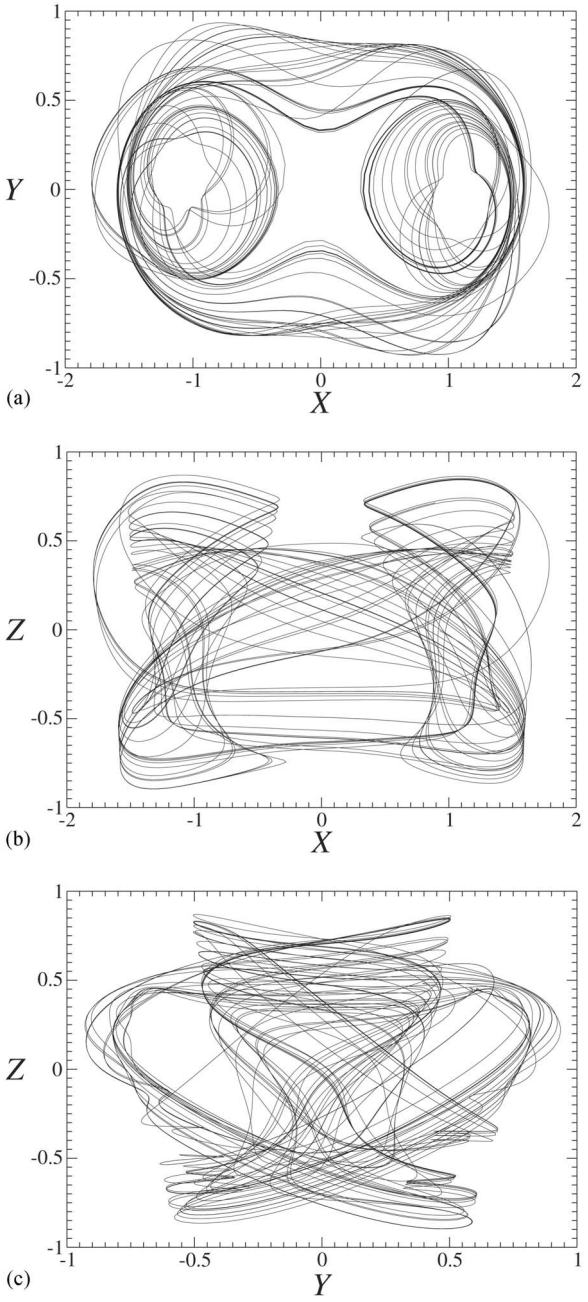

FIG. 13. Double cover of the chaotic attractor solution of Eq. (3) for the Shaw version of the van der Pol equations is mapped from $D^2 \times S^1$ by a natural embedding. The center line of the torus is mapped to a circle of radius 1.2 in the x-y plane. A correlated peeling bifurcation occurs when the double cover is around the twofold rotation axis through $(x,y)=(1.2,0.0)$. The three images are projections onto the X-Y, X-Z, and Y-Z planes, from top to bottom.

The attractor is mapped into $\mathbb{R}^3$ following the prescription $x(t)=[\rho-u(t)]\cos(\omega t), y(t)=[\rho-u(t)]\sin(\omega t), z(t)=v(t)$, with $\rho=1.2$. This flow, embedded in $\mathbb{R}^3$, has the topology of a hollow donut. A projection onto the x-y plane is shown in Fig. 12.

The covers of the chaotic attractor produced by this embedding into $\mathbb{R}^3$ undergo correlated peeling bifurcations as the rotation axis slices through the image. In Fig. 13 we

show three projections of the double cover obtained when the symmetry axis is parallel to the Z axis and has twofold symmetry. The rotation axis passes through the point $(x,y)=(1.20,0.0)$ in the x-y plane. The continuous version of this correlated peeling bifurcation is available in [16].

Both this attractor and the Lorenz attractor are contained in genus-three bounding tori. The two attractors are topologically inequivalent. The X-Y projection of this attractor, which is shown in Fig. 13(a), is similar to the X-Y projection of the Lorenz attractor. However, projections onto the other two directions are totally different. The toroidal structure of the present attractor is revealed in the projections shown in Figs. 13(b) and 13(c). A Poincaré section of the double cover of the van der Pol attractor (Fig. 14) shows the double annular shape. The two components of the Poincaré surface of section consist of two half planes, both with $Y=0$. One is hinged on an axis parallel to the Z axis through $(X,Y)=(1.1,0)$; the other is the rotation image of the first. Intersections with $Y=0$, $\dot{Y}>0$ are taken on one half-plane and intersections with $Y=0$, $\dot{Y}<0$ are taken with the other. This Poincaré section emphasizes the invariance of this attractor under rotation symmetry around the Z axis.

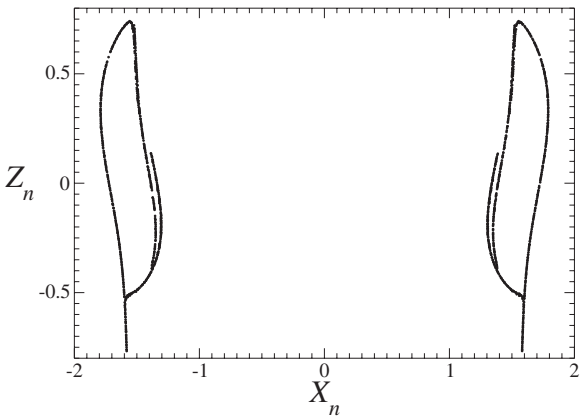

FIG. 14. Intersections of the double cover (Fig. 13) of the van der Pol attractor with the two disconnected components of the Poincaré section. The component on the right has $Y=0$, $X>+1.1$ with $\dot{Y}>0$ and the component on the left has $Y=0$, $X<-1.1$ with $\dot{Y}<0$. The rotation symmetry is clear.

VII. SUMMARY

It is remarkable that the global topology of the image attractor imposes nontrivial constraints on its properties and those of its covers. Specifically, an attractor whose phase space is a hollow donut intersects a rotation axis an even number of times (more precisely, its branched manifold does). Further, its branched manifold can have only an odd number of branches. These remarkable properties extend, in a suitable way, to double covers of these attractors.

Methods for constructing double covers of chaotic attractors have been applied to chaotic attractors of a toroidal nature. These attractors are contained in genus-one bounding tori and are described by branched manifolds with a circular cross section on a Poincaré surface of section [9]. Their return maps are maps of the circle to itself. Their double covers are created by correlated peeling bifurcations. The morphology of the covering attractor changes systematically as the rotation symmetry axis slices through the image torus from outside to inside. Outside, the double cover consists of two identical attractors, each contained in a genus-one torus. The two genus-one tori are disconnected. When the rotation axis intersects the image, the double cover is contained in a genus-three torus, and is not structurally stable against perturbations of the position of the rotation axis. When the rotation axis enters the hole in the torus, the double cover exists in a genus-one torus. For various ranges of lift parameter values rotations can appear to occur around a single center, two centers, or three centers. Lifts of periodic orbits in the image attractor are described by a powerful synthesis of kneading theory with refinements of the circle map.

ACKNOWLEDGMENT

R.G. thanks the CNRS for an invited position at CORIA for 2006–2007.

[1] R. Miranda and E. Stone, Phys. Lett. A **178**, 105 (1993).
[2] C. Letellier and R. Gilmore, Phys. Rev. E **63**, 016206 (2000).
[3] R. Gilmore and C. Letellier, Phys. Rev. E **67**, 036205 (2003).
[4] R. Gilmore and C. Letellier, *The Symmetry of Chaos* (Oxford, NY, 2007).
[5] C. Letellier and R. Gilmore, J. Phys. A **40**, 5597 (2007).
[6] E. N. Lorenz, J. Atmos. Sci. **20**, 130 (1963).
[7] O. E. Rössler, Phys. Lett. **57A**, 397 (1976).
[8] R. Gilmore, Rev. Mod. Phys. **70**, 1455 (1998).
[9] R. Gilmore and M. Lefranc, *The Topology of Chaos* (Wiley, NY, 2002).
[10] J. S. Birman and R. F. Williams, Topology **22**, 47 (1983).
[11] J. Birman and R. F. Williams, Contemp. Math. **20**, 1 (1983).
[12] T. D. Tsankov and R. Gilmore, Phys. Rev. Lett. **91**, 134104 (2003).
[13] T. D. Tsankov and R. Gilmore, Phys. Rev. E **69**, 056206 (2004).
[14] O. E. Lanford, *Circle Mappings*, in *Recent Developments in Mathematical Physics*, edited by H. Mitter and L. Pittner (Springer-Verlag, Berlin, 1987), pp. 1–17.
[15] C. Letellier, T. D. Tsankov, G. Byrne, and R. Gilmore, Phys. Rev. E **72**, 026212 (2005).
[16] http://lagrange.physics.drexel.edu/flash/td2 and http://lagrange.physics.drexel.edu/flash/tofu
[17] R. Shaw, Z. Naturforsch. A **36**, 80 (1981).